High Isp Mechanism of Rectangular Laser-Electromagnetic Hybrid Acceleration Thruster

IEPC-2011-274

Presented at the 32nd International Electric Propulsion Conference,
Wiesbaden • Germany
September 11 – 15, 2011

Hideyuki Horisawa[1], Yuki Mashima[2], Osamu Yamada[3]
Dept. Aeronautics and Astronautics, Tokai University, Hiratsuka, Kanagawa, 259-1292, Japan

and

and Ikkoh Funaki[4]
JAXA/ISAS, Sagamihara, Kanagawa, 252-5210, Japan

Abstract: A fundamental study of a newly developed rectangular pulsed laser-electromagnetic hybrid thruster was conducted. Laser-ablation plasma in the thruster was induced through laser beam irradiation onto a solid target and accelerated by electrical means instead of direct acceleration only by using a laser beam. The performance of the thrusters was evaluated by measuring the mass shot and impulse bit. As results, significantly high specific impulses up to 7,200 sec were obtained at the charge energies of 8.6 J. Moreover, from the Faraday cup measurement, it was confirmed that the speed of ions was accelerated with addition of electric energy.

I. Introduction

THE current trend towards smaller spacecraft, which is not only mass limited but also power limited, has produced a strong interest in development of micropropulsion devices.[1-4] The significance in reducing launch masses has attracted growing interests in regard to reduction of mission costs and increase of launch rates. Although, in the past, many very small spacecraft have lacked propulsion systems altogether, future microspacecraft will require significant propulsion capability in order to provide a high degree of maneuverability and capability. The benefit of using electric propulsion for the reduction of spacecraft mass will likely be even more significant for mass limited microspacecraft missions.[2] Feasibility studies of microspacecraft are currently under development for a mass less than 100 kg with an available power level for propulsion of less than 100 watts.[2-4] Various potential propulsion systems for microspacecraft applications have been proposed and are under significant development for primary and attitude control applications.[4]

On the other hand, small-sized onboard laser plasma thrusters are also under significant development with rapid evolutions of novel compact laser systems. One of the advantages of the laser thrusters is that they can induce high specific impulse. In addition, the system can be very simple and small with significant controllability of the thrust.[5-12] In order to improve thrust performances and system simplicities of those conventional electric and laser propulsion systems, a preliminary study on a laser-electric hybrid propulsion system was conducted.[13-15] A basic idea of these systems is that a bunch of laser-ablation plasma, induced through laser irradiation on a solid target, is additionally accelerated by electrical means. Since any solid material can be used for the propellant in these cases, no tanks, no valves, or piping systems are required for the propulsion system. Also, various materials in any phase

---

[1] Professor, Department of Aeronautics and Astronautics, horisawa@tokai.ac.jp
[2] Graduate Student, Department of Aeronautics and Astronautics
[3] Graduate Student, Department of Aeronautics and Astronautics, hikohikootsukare@gmail.com
[4] Associate Professor, Institute of Space and Astronautical Science, funaki@isas.jaxa.jp

can be used for the propellant. Therefore, the system employing this technique can be simple and compact. As the laser-ablation plasma has a directed initial velocity of tens of km/sec, which will be further accelerated by electrical means, significantly high specific impulses can be expected.

Depending on electrode configuration, plasma density, electrical input-power (voltage and current), etc., acceleration mechanisms for the laser-ablation plasma can be varied into three types, i.e., i) electrostatic acceleration, ii) electromagnetic acceleration, and iii) electrothermal acceleration. Especially for the laser-ablation plasma, depending on laser conditions such as pulse energy, fluence, etc., plasma density distribution can be widely controlled. Moreover, this can also be increased through additional electric discharges.

A schematic of the rectangular laser-electromagnetic hybrid accelerator is illustrated in Fig.1. It utilizes laser-beam irradiation to induce plasma ionized from a solid propellant between electrodes, and then an electric discharge is induced in this conductive region. As the current running between the anode and cathode is increased, the plasma can be heated and further ionized through Joule heating. Thus, the electrothermal acceleration effect becomes significant. When current exceeds more than one thousand amperes, an electromagnetic acceleration effect becomes significant. With interaction of the current and self-induced magnetic field, a streamwise acceleration is provided.[16,17]

Because the use of a shorter laser pulse enables a shorter pulsed-plasma generation, a significantly high peak current can be induced. Since the force induced in the accelerator is dependent on the square of the current, significant improvements in acceleration characteristics can be expected. In addition, depending on laser power, laser-induced plasma produced from a solid propellant usually has a directed initial velocity, and this can also contribute to an improvement in the acceleration performance.

In this study, to optimize the geometry of the acceleration channel and propellant material, thrust performance of the accelerators, or thrusters, with various channel geometries and propellant materials was experimentally estimated and compared through the measurements of impulse-bit and propellant consumption rate.

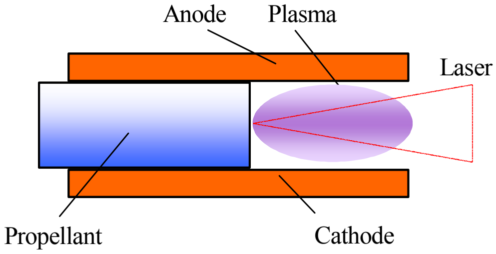

(a) Schematic illustration.

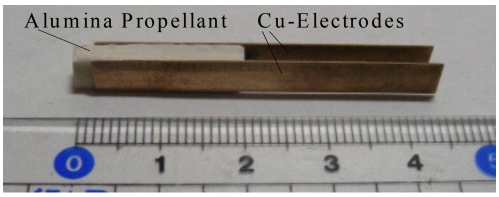

(b) Photo of the thruster.

Figure 1. Schematic illustration and photo of a rectangular laser-electromagnetic hybrid thruster.

II. Experimental

A schematic illustration of laser-electromagnetic hybrid acceleration system is shown in Fig.1. The thruster utilizes a laser-beam assistance to induce a bunch of plasma, ionized from a solid-propellant between electrodes, and then an electric discharge is induced in this conductive region. Since the plasma is induced through the laser ablation of the solid propellant in this system, various substances, such as metals, polymers, ceramics, etc., in various phases can be used for the propellant. Therefore, this system must be effective not only for space propulsion devices but also for plasma sources in material processing in industrial applications. For a rectangular laser-electromagnetic hybrid acceleration system, a pair of copper electrodes and a solid propellant, alumina (Al_2O_3), with various sizes of the acceleration channel, were used.

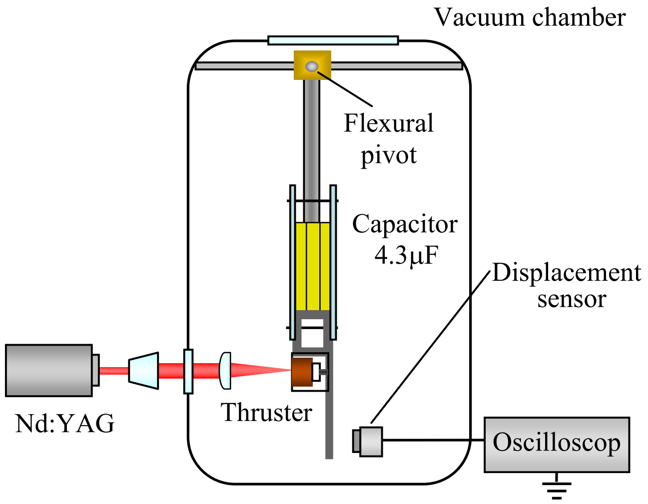

Figure 2. Schematic of experimental setup for measurement of an impulse bit.

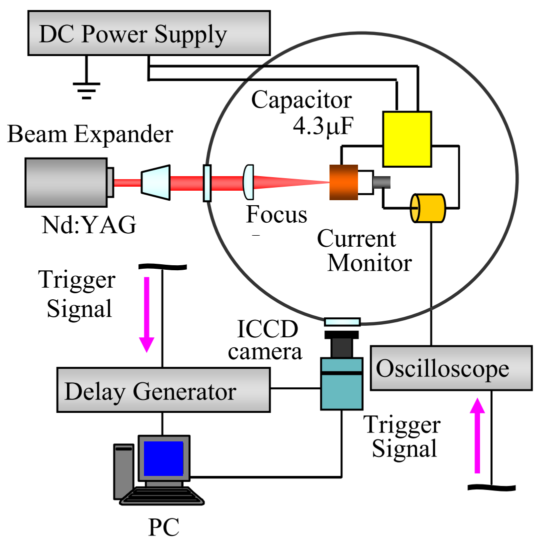

Figure 3. Schematic of experimental setup for ICCD camera observation.

Schematics of experimental setups are illustrated in Figs.2 to 4. A Q-switched Nd:YAG laser (BMI, 5022DNS10, wavelength: λ = 1,064 nm, pulse energy: 266 mJ/pulse, pulse width: 10 nsec) was focused with a focusing lens (f = 100 mm) and irradiated on a propellant surface to induce a laser ablation plasma supplied as a bunch of plasma propellant to the acceleration channel. As shown in this figure, the laser pulse was irradiated from the outside of the vacuum chamber (10^{-3} Pa) through a quartz window.

In this study, to verify the effect of acceleration channel geometry on thrust performance, various sizes of the acceleration channel, i.e., length, height, and width, were prepared and tested. Sizes of the acceleration channel examined in this study are listed in Table 1.

To characterize propulsive performance of the various acceleration systems, impulse-bit measurement and mass shot measurement were experimentally conducted, and from these values specific impulse and thrust efficiency were calculated and compared. A torsion-balance thrust stand, shown in Fig.2, was used for the impulse-bit measurement. It consists of a balance, a pair of pivots, and a displacement sensor. The balance is 450 mm long made and is made of aluminum. Distance between the pivot and thruster is set to 437 mm. For the pivots, the Flexural Pivot (SDP/SI) was used. The torsional spring rate of the pivot used in this experiment is k = 4.7 x 10^{-2} Nm/rad. As for the displacement sensor, an eddy current displacement sensor (EMIC, 503-F, NPA-010, maximum range: 1 mm, minimum displacement: 0.5 μm) located at 450 mm from the pivots was used. Calibration of the torsion-balance was conducted with known impulses using arbitrary impacts of an aluminum ball of 187 mg suspended by a string of 370 mm in length. Assuming a perfect inelastic collision of the ball with the balance, known impulses could be given to the balance, and then displacements of the balance were monitored.

For the measurement of a mass-shot per pulse-shot of the propellant, or propellant consumption rate per shot, we used an electronic precision balance (Shimazu AUX220, accuracy: 0.1 mg). The typical number of pulse-shots to measure the mass-shot was 5,000 times. In addition, the mass-shots were also estimated from the measurement of removed volumes of the propellant target surface after the number of shots, where the volume was measured by the vision measuring system (Mitsutoyo, QV-APEX302).

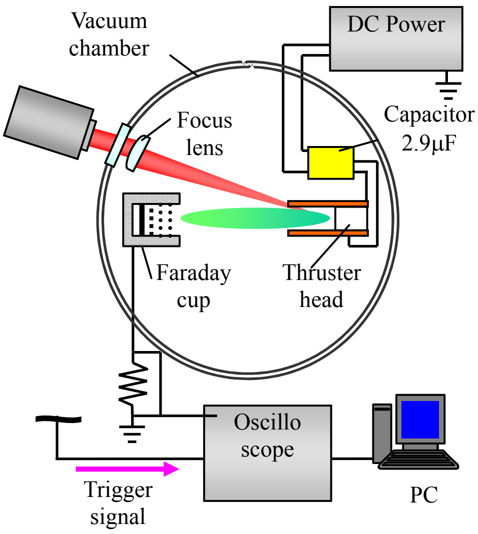

Figure 4. Schematic of experimental setup for Faraday cup measurement.

Table 1. Sizes of acceleration channels tested in this study.

Electrode height	Channel length	Width
3.0mm	10, 50mm	5.0mm
5.0mm	10, 30, 50mm	5.0mm
10.0mm	10, 50mm	5.0mm

Plasma behaviors were observed with an ICCD camera (minimum gate width: 2 nsec), shown in Fig,3. Generating an arbitrary delay with a delay generator trigerred by a Q-sw output signal, the ICCD camera was synchronized with a laser pulse. Since this phenomenon was highly reproducible, it was possible to obtain images of a temporal growth of a plasma formation process with 2nsec resolution through changing the delay timing. Images from the ICCD camera were processed into colored contour lines proportional to the emission intensity distribution with an image processing code (MEDIA CYBERNETICS, Image Pro Plus).

Temporal evolutions of ion current were observed with a Faraday cup, shown in Fig.4. The Faraday cup consisting of stainless grids of 400 mesh/inch and 10 mm in diameter was placed at 210 mm away from the bottom of the thruster aligned in the center line of the plume. The ion currents were monitored by an oscilloscope (LeCroy, 9374TM, range: 1 nsec/div ~ 5 msec/div). Estimating the time-of-flight of ions, where time of arrival of the most part of the ions was presumed as that of the maximum current.

III. Results and Discussion

A. Influence of Electrode Geometries on Thrust Performance

Variations of impulse-bit with charge energy are plotted in Fig.5 for various electrode geometries. From the figure, it can be seen that impulse-bit increased with charge energy in all the cases. Comparing the effect of electrode length among electrode height of 5 mm (i.e., 5x10, 5x30, 5x50), the longest 5x50 thruster with the length of 50 mm showed the highest impulse-bit. From this result, the importance of electrode length, or acceleration channel length, was confirmed.

Effect of the channel height with constant lengths of 10 mm and 50 mm can be seen by comparing the 3x10, 5x10, 10x10, and 3x50, 5x10, 10x10 thrusters. In the thrusters with shorter channel length of 10 mm, the 5x10 thruster with the height of 5 mm showed higher impulse-bit than those with 3 mm and 10 mm. On the other hand, with longer channel length of 50 mm, the 10x50 thruster with largest width showed the highest impulse-bit.

Although not shown, mass shots of alumina propellant were significantly smaller than those of BN and PTFE. Typical values of the mass shot of the alumina propellant varied from 0.34 to 0.42 μg/pulse for charge energy of from 2.15 to 8.60 J. With its superior corrosion resistance and higher melting point, the mass loss of alumina due to the thermal influence of the discharge plasma could be significantly limited, resulting in significantly high specific impulse and thrust efficiency.

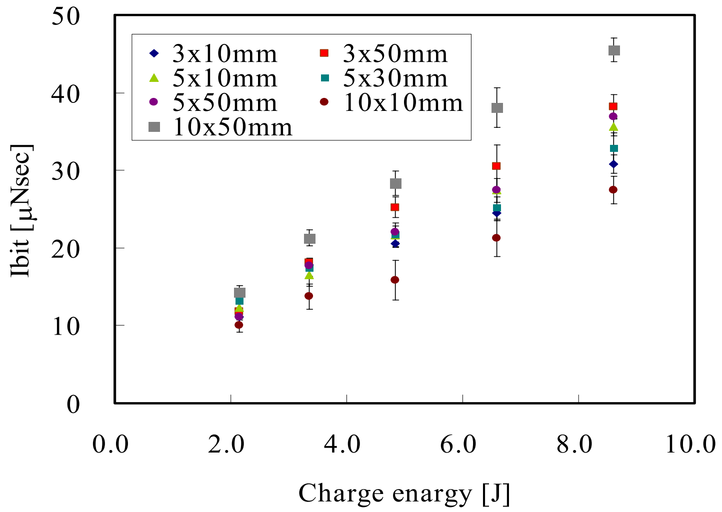

Figure 5. Variations of impulse bits with charge energies for thrusters with various electrode geometries.

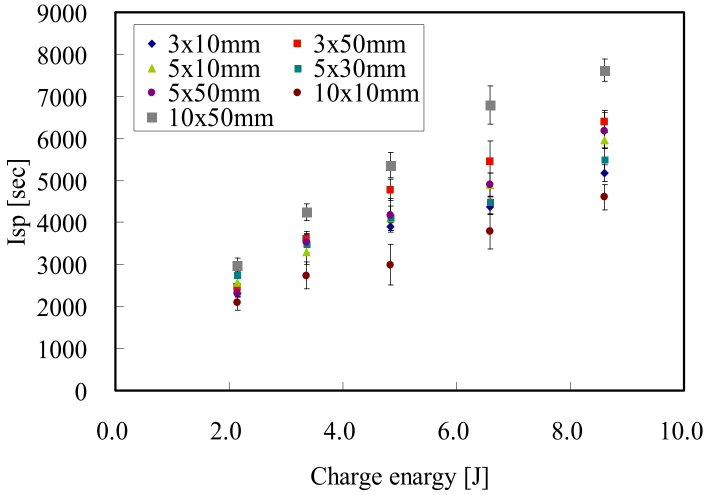

Figure 6. Variations of specific impulse with charge energies for thrusters with various electrode geometries.

Variations of specific impulse with charge energy are plotted in Fig.6 for various acceleration channel configurations. From the figure, it can be seen in all the cases that specific impulse increased with the increase of the charge energy. Moreover, thrusters with longer channel length showed higher specific impulses. The highest specific impulse of 7,200 sec was obtained with the 10x50 thruster at the highest charge energy of 8.6 J.

Considering the thrust generation theory of the conventional pulsed plasma thrusters (PPTs), integrating electromagnetic force in a whole volume of the acceleration channel, higher impulse-bit can be obtained in thrusters with larger channel volume, i.e., the 10x50 thruster. However, with the shorter length the decrease of the impulse-bit was observed in larger width cases. Since the laser ablation plasma occurs from a focal point of the laser beam without radially spreading, the discharge current cannot run efficiently between the electrodes if the thruster has wide and short acceleration channel. From these facts, it was shown that further optimization of the geometries of the acceleration channel should be conducted for the next step of this study.

B. Ion Emission Characteristics

Temporal variations of ion currents exhausted from the thruster measured with a Faraday cup are shown in Figs.7 and 8 for low and high energy cases charged to the thruster, respectively. Although coupled with large noise signals in Fig.7, it can be seen that values of peak currents for various voltage cases decrease and temporal positions of the peaks shift toward shorter times with increase of the voltages, or charge energies. For 0 V, the position of the peak is about 8 μsec, 300 V. On the other hand for 300 V, the position of the peak is about 6.6 μsec.

Results for higher voltage cases, or charge energies, are shown in Fig.8, where an ion current wave of 0 V magnified by 5 times is also shown for comparison. As shown in this figure, with higher voltages or charge energy cases, temporal positions of the peaks become shorter, i.e., 5 μsec for 1,000 V (charge energy of 1.4 J). From these results, calculated speed of ions roughly estimated form these times and distance (210 mm) are 25 km/sec and 42 km/sec for 0 J and 1.4 J cases, respectively. It is therefore confirmed that the speed of ions is accelerated with addition of electric energy. Although for higher voltage cases, over 1,000 V, positions of the peaks are not becoming shorter, values of the peak currents are increasing with increase of voltages. From these results, it is confirmed that number of ions entering the Faraday cup is increasing with increase of voltages, or charge energies.

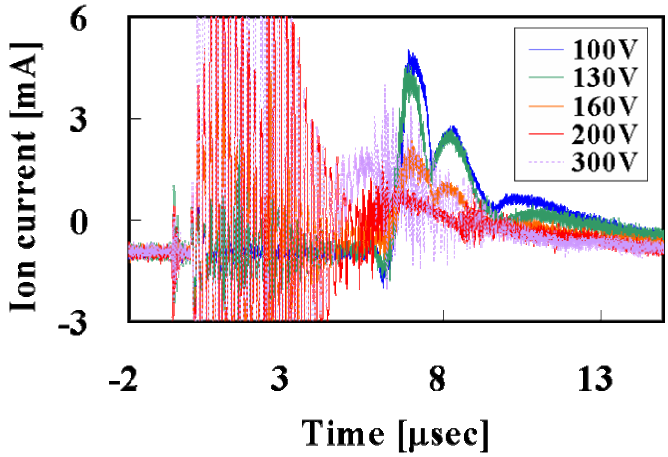

Figure 7. Temporal variation of ion current for low charge voltage cases.

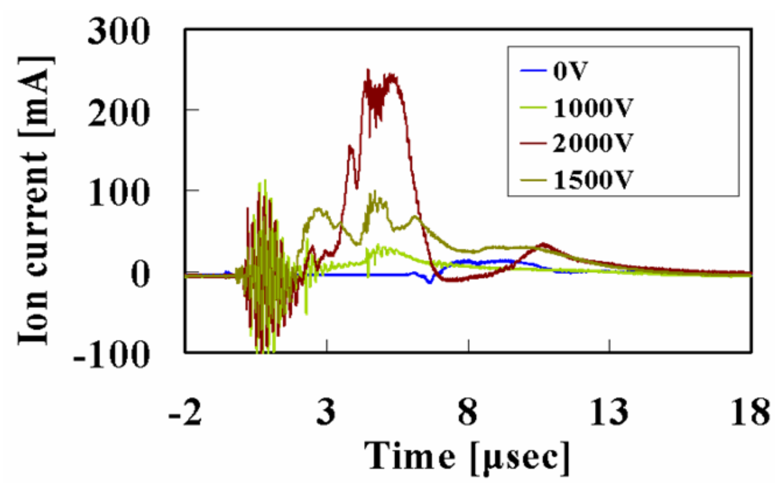

Figure 8. Temporal variation of ion current for high charge voltage cases.

From the typical speed of ions of 42 km/sec at charge energy of 1.4 J, a specific impulse estimated from the division of the speed by the gravitational acceleration (9.8 m/sec^2) is *I*sp = 4,290 sec. On the other hand, extrapolation of specific impulse data measured from the impulse and mass shot measurements shown in Fig.6 at 1.4 J will give *I*sp ~ 2,000 sec. This large discrepancy of specific impulses is mainly due to the measurement of only fast ions and exclusion of contribution of neutral species in Faraday cup measurement. Since the ion speed estimated from the ion current of the Faraday cup is only measuring the signal of ions included in the exhausted plasma plume, effects of other species such as neutral atoms, molecules, and particles, which are much slower than those ions in most cases, are not included.

C. Plasma Behavior Characterization with ICCD Camera

ICCD images of a discharging plasma plume exhausted from the thruster are shown in Figs.9 and 10, for 0 and 2000 V cases, respectively. After laser irradiation, a small spot plasma at the center of an exposed propellant surface is induced. Comparing these figures, it can be seen that plasma behaviors are similar between those three cases up to 500 nsec.

In Fig.10, for 2000 V case with a lager capacitor to enhance an electromagnetic acceleration effect, canted current sheet structures can be seen from 1000 to 1500 nsec, when the current reaches the first positive peak and an associated electromagnetic effect probably becomes significant. Here, the plasma of anode side is moving faster than that of cathode side. Then the current reaches the first negative peak at 4500 nsec, in which the plasma of cathode side is faster than anode side, the second positive peak at 7500 nsec, and the second negative peak at 10500 nsec.

From these results, it is found that discharge durations at low-voltage cases (~ 40 V) are as long as those of laser-induced plasmas. Therefore, the discharge in the low-voltage case must be controlled with the incident laser pulse, or laser-induced plasma. While in high-voltage cases, discharge durations are much longer than those of laser-induced plasmas. In this case, the laser-induced plasma should be leading a main discharge from a capacitor, where some amount of neutral components of vaporized propellant must be ionized through the main discharge.

Although motion of the plasma plume is not clearly obtained in each image, speeds of the plasma can be roughly calculated by estimating temporal variations of displacements of the plume in these images. From the estimation the speed varied from 30 to 50 km/sec. Further estimation should be additionally done for detailed measurement of the speed.

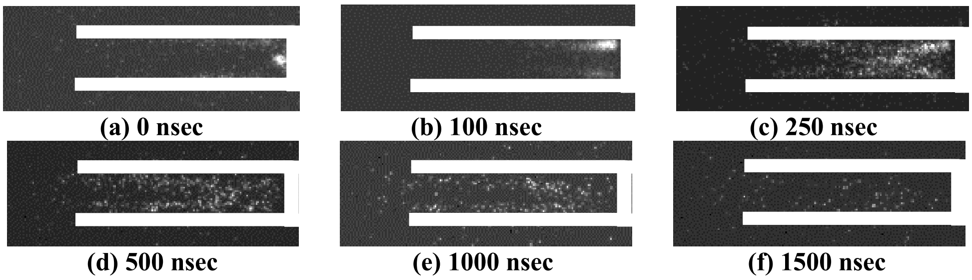

Figure 9. ICCD images of plume from a rectangular thruster (anode: upper plate) for 0V.

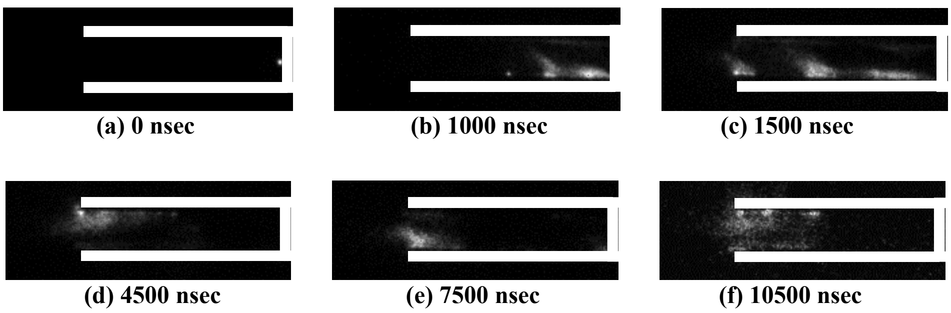

Figure 10. ICCD images of plume from a rectangular thruster (anode: upper plate) for 2000V.

IV. Conclusion

In this study, experimental investigation of measurement of impulse-bit and propellant consumption rate, or mass shot, per single pulse discharge was conducted to characterize the thrust performance of the rectangular laser-electromagnetic hybrid acceleration thruster with alumina propellant. In addition, the thrust performance was measured in seven thrusters with different channel lengths and electrode intervals to investigate the influence of acceleration channel geometry. The impulse-bit and specific impulse obtained with the smallest 3x10 thruster varied from 10 μNsec to 28 μNsec and from 2,100 to 4,600 sec for the charge energy of 2.15 to 8.6 J. In addition, the typical values of impulse-bit and specific impulse obtained with the largest 10x50 thruster varied from 14 μNsec to 45 μNsec and from 3000 to 7,200 sec for the charge energy of 2.15 to 8.6 J. It was confirmed that higher electromagnetic effect could be obtained in larger volume of the acceleration channel.

Moreover, an investigation on behavior of plasma plume was conducted with Faraday cup and ICCD camera. From the Faraday cup measurement, it was confirmed that the speed of ions was accelerated with addition of electric energy. From the ICCD camera observation, motion of the plasma in the acceleration channel was characterized.

References

[1] Myers, R.M., et al., "Small Satellite Propulsion Options," AIAA Paper 94-2997, June 1994.

[2]Mueller, J., "Thruster Options for Microspacecraft: A Review and Evaluation of Existing Hardware and Emerging Technologies," AIAA Paper 97-3058, July 1997.

[3]Leifer, S., "Overview of NASA's Advanced Propulsion Concepts Activities," AIAA Paper 98-3183, July 1998.

[4]Micci, M. M., and Ketsdever, A. D. (ed.), *Micropropulsion for Small Spacecraft*, American Institute of Aeronautics and Astronautics, USA, 2000.

[5]Phipps, C., and Luke, J., "Diode Laser-Driven Microthrusters: A New Departure for Micropropulsion", *AIAA Journal*, Vol.40, No.2, 2002, pp.310-318.

[6] Gonzales, D., and Baker, R., "Micropropulsion using a Nd:YAG Microchip Laser," *Proceedings of SPIE*, Vol.47,No.60, 2002, pp.752 – 765.

[7]Pakhomov, A.V., et al., "Specific Impulse Study of Ablative Laser Propulsion," AIAA Paper 2001-3663, 2001.

[8]Horisawa, H., and Kimura I., "Fundamental Study on Laser Plasma Accelerator for Propulsion Applications," *Vacuum*, Vol.65, No.3-4, 27 May 2002, pp.389-396.

[9]Phipps, C., et al., "Review: Laser-Ablation Propulsion," *Journal of Propulsion and Power*, Vol. 26, No.4, 2010, pp.609-637.

[10]Pakhomov, A.V., Thompson, M., Swift Jr., W. and Gregory, D.: Ablative Laser Propulsion: "Specific Impulse and Thrust Derived from Force Measurements," *AIAA Jurnal*, Vol.40, 2002, pp.2305-2311.

[11]Phipps, C. R., Luke, J., Lippert, T., Hauer, M. and Wokaun A.: "Micropropulsion Using a Laser Ablation Jet," *J. Propulsion and Power*, Vol.20, 2004, pp.1000-1011.

[12]Phipps, C. R., Luke, J. and Helgeson, W. D.: "3ks Specific Impulse with a Nspulse Laser Microthruster," Proc. 29th Intl. Electric Propulsion Conf., IEPC 319 (CD-ROM), 2005.

[13]Horisawa, H., Kawakami, M., Kimura, I., "Laser-assisted pulsed plasma thruster for space propulsion applications," *Applied Physics* A, Vol.81, 2005, pp.303 − 310.

[14]Horisawa, H., Sasaki, K., Igari, A., and Kimura, I., "Laser-Electric Hybrid Acceleration System for Space Propulsion Applications," *The Review of Laser Engineering*, Vol.34, 2006, pp.435- 441.

[15]Ono, R. G. Jahn, Physics of Electric Propulsion, McGraw-Hill, 1968, pp.198-316.T., Uchida, Y., Horisawa, H., and Funaki, I., "Measurement of ion acceleration characteristics of a laser-electrostatic hybrid microthruster for space propulsion applications," *Vacuum*, Vol.83, 2008, pp.213-216.

[16]Jahn, R. G., *Physics of Electric Propulsion*, McGraw-Hill, 1968, pp.198-316.

[17]Burton, R. L., and Turchi, P. J., "Pulsed Plasma Thruster," *Journal of Propulsion and Power*, Vol. 14, 1998, pp.716–735.